

# The Effect of Using DMSO as a Cosolvent for Ligand Binding Studies

**Simon Birgersson**

---

Master Thesis in Biophysical Chemistry, 2018

Department of Chemistry

Lund University

Sweden





# The Effect of DMSO on Binding Affinity

Simon Birgersson



**LUND**  
UNIVERSITY

## MASTER'S THESIS

Master of Science in Engineering, Biotechnology  
Faculty of Engineering  
Lund University, Sweden  
2018-02-01

## SUPERVISORS

Mikael Akke, Olof Stenström

## EXAMINER

Kristofer Modig

Division of Biophysical Chemistry  
Department of chemistry  
Faculty of Engineering  
Lund University, Sweden

## Abstract

DMSO sees common application as a solvent for studies of synthetic molecules in biological systems, in fields such as drug design. Despite this, the possibility and nature of solvent interactions with both synthetic ligand and their target macromolecules is widely unexamined. DMSO could potentially have significant effect on binding characteristics due to conformational changes of protein structure. In this thesis, I have studied the effects of DMSO on the binding of a synthetic ligand to the carbohydrate recognition domain of galectin-3C using isothermal titration calorimetry (ITC) and NMR relaxation dispersion experiments. ITC reports on the thermodynamics of binding, whereas NMR relaxation dispersion reports on the kinetics of binding. ITC results displayed an increase in calculated  $K_D$  from 5.588  $\mu\text{M}$  to 13.02  $\mu\text{M}$  with the addition of 10 % (v/v) DMSO, as well as an increase in free energy from  $-30.28$  kJ/mol to  $-28.1665$  kJ/mol. NMR relaxation dispersion studies showed that the chemical exchange rate of binding site residues decreased as well. Kinetic on- and off-rates were determined from the chemical exchange rate. Notably the on-rate was affected by DMSO  $\sim 10\%$  more than the off-rate, indicating that the reduced binding affinity is primarily caused by a reduced frequency of protein-ligand encounters.

## Sammanfattning

DMSO är ett vanligt lösningsmedel för studier av syntetiska molekyler i biologiska system, bl.a. inom läkemedelsutveckling. Trots detta är lösningsmedlets interaktioner med dessa syntetiska molekyler och deras målprotein inte tillräckligt undersökta. DMSO kan påverka proteinerna struktur eller ha någon annan inverkan inbindningen. I detta arbete har denna möjliga effekt studerats för inbindningen av den syntetiska molekylen KP0440 och en kapad version av proteinet Galectin-3 som endast innefattar the kolhydratsbindande domänet. Detta utförs med hjälp av ITC och CPMG relaxations-dispersionsexperiment för att utvärdera inverkan på både termodynamiska och kinetiska parametrar över en spädningsserie DMSO från 0 % till 10 % volymprocent. Resultaten från ITC visade en ~60% försvagad inbindning vid tillsättning av 10 % DMSO och en mer gynnsam entropi för liganden fritt i lösningen än jämfört med i bundet tillstånd när DMSO var tillsatt. CPMG-studierna visade att det kemiska utbytet mellan bundet och obundet tillstånd minskade med DMSO på ett liknande vis som hos ITC-resultaten. Kinetiska på- och av-hastigheter räknade ut utifrån kemiska utbyteskonstanten, och av intresse var att minskningen var större för på-hastigheten relativt till av-hastigheten vilket skulle innebära att DMSO:s inverkan skulle mest bero på den minskade frekvensen av mötet mellan protein och ligand i lösningen.

## Acknowledgements

The thesis project has been carried out between 10/9-18 and 1/2-19 at the Division of Biophysical Chemistry at Lunds Tekniska Högskola (LTH) in order to discern and characterize the effect of using dimethyl sulfoxide (DMSO) on protein binding in terms of affinity. The work has been supported by, and wouldn't have been possible without the help of supervisor Mikael Akke, assistant supervisor Olof Stenström as well as Sven Wernerson, Kristine Steen and Johan Wallerstein who helped me with many aspects of this project. I would also like to thank Kristofer Modig for helping examining the project, Soumendranath Bhakat and Pär Söderhjelm for their technical support, as well as Ulf Nilsson and the people at CAS for their assistance in synthesis and formulation of the ligand used for this project. Lastly, I would like to thank my friends and family for all the support.

## Populärvetenskaplig sammanfattning - Molekylernas mikroskopiska värld och läkemedelsutvecklingens framtid

Protein är livets arbetshästar. Nästan varje liten sak som händer i kroppen, från synen, till matsmältningen, till allt annat sker med hjälp av proteiner. Galectin-3 är ett protein i människokroppen som binder till socker. Man tror att galectin-3 är inblandat i många sjukdomar, men är allra mest inblandad i cancerutveckling. Därför är det väldigt intressant att studera olika sätt att utveckla läkemedel som binder till detta protein. Med hjälp av olika tekniker kan man studera på mikroskopisk nivå hur det här proteinet ser ut och hur mycket den tycker om att reagera med olika möjliga syntetiska molekyler. Men när man studerar dessa olika molekyler är det viktigt att allting betar sig som man förväntar sig att det kommer att göra när det sker på riktigt i människokroppen, men detta kan vara svårare än man tror.

Mitt examensarbete har handlat om att undersöka om ett speciellt ämne dimetylsulfoxid, eller DMSO, har någon inverkan på själva resultatet av en typisk sådan här studie. DMSO hjälper till att få ämnen som vanligtvis inte kan lösa sig i vatten att göra det, vilket kan vara väldigt hjälpsamt när man vill undersöka nya konstiga molekyler. Enligt nya rön har det visat sig att detta lösningsmedel kan påverka proteinet, vilket inte alls är bra! Men hur ska man undersöka något så litet som hur ett protein kläms ihop av en molekyl som är ännu mindre? När man studerar saker på mikroskopisk skala fungerar det sällan att försöka få fram bilder, utan man får istället försöka att få en uppfattning genom att studera andra saker. En av metoderna som jag använt heter ITC, där mäter man den oerhört lilla värme som släpps fri eller tas upp när man tillsätter en av delarna i en reaktion till den andra. Med hjälp av denna energi kan man uppskatta hur mycket proteinet vill binda sockermolekylen vilket är väldigt bra om man vill ta fram en ny molekyl.

Den andra metoden jag använde heter NMR, som istället mäter magnetismen i molekylerna för att få reda på om dem. NMR fungerar som magnetröntgen ungefär, fast man försöker få en bild av små molekyler istället för insidan av människokroppen. Det häftiga med detta är att man kan undersöka händelser som händer över tid! Med detta kan man till exempel se hur ett protein ändrar på sig när det binder till en sockermolekyl, och vad som händer sen när sockret släpper igen. De här är metoder som kan användas för enormt många olika saker, och därför tycker jag det är viktigt att man vet vad det är man undersöker när man utför dem. I mitt projekt visade resultaten att det faktiskt fanns en effekt, mest relaterat till att lösningen blev mer trögflytande med DMSO i vilket gör det svårare för sockermolekylerna att ta sig fram igenom lösningen, lite som att försöka simma i en gröt! Detta är alltså något man måste ha i åtanke när man designar framtida läkemedel, som kan till exempel tillåta oss att bekämpa cancer utan skadlig kemoterapi.

# Table of Contents

Background	7
Introduction	7
Isothermal Titration Calorimetry	7
Basic Concept of Nuclear Magnetic Resonance Spectroscopy	8
CPMG	9
Dimethyl Sulfoxide	11
Galectin-3C	11
KP0440	11
Aim of the study	12
Materials and Method	12
Instruments	12
Procedure	12
Protein preparation	12
Determination of protein concentration	12
Preparation of sample solutions	13
Protein and ligand concentrations	13
Preparation of DMSO dilution series for ITC experiment	13
Preparation of NMR samples	13
ITC measurement	14
Data analysis of ITC measurements	14
NMR	14
Results	15
ITC measurements	15
NMR	17
Discussion	20
Conclusions	21
References	23
Appendix	25
Appendix A - Thermograms	25
Appendix B - CPMG relaxation Dispersions	39



## List of Abbreviations

---

Abbreviation:	Explanation:
ITC	Isothermal Titration Calorimetry
NMR	Nuclear Magnetic Resonance
FID	Free Induction Decay
HSQC	Heteronuclear Single Quantum Coherence
CPMG	Carr-Purcell-Meiboom-Gill
DMSO	Dimethyl Sulfoxide
Gal-3	Galectin-3
Gal-3C	Truncated version of Galectin-3
CRD	Carbohydrate Recognition Domain
HEPES	4-(2-hydroxyethyl)-1-piperazineethanesulfonic acid
KP0440	Ligand used for the project
PDB	Protein Data Bank
NOE	Nuclear Overhauser Effect

---

# Background

## Introduction

Biological assays that discern thermodynamic properties of biological systems are of great importance to fields such as drug design, nanotechnology and polymer chemistry (Bouchemal et al., 2008). Isothermal Titration Calorimetry (ITC) is a common method used for characterizing molecular interaction in order to determine binding affinity, an important aspect of designing effective functional molecules. In these assays DMSO sees application as a polar aprotic agent (Sigma Aldrich, 2018) used for solvation of organic ligands. According to previous literature, addition of DMSO in protein-ligand binding studies has displayed a decrease in affinity (Cubrilovic et al, 2013). Potential misrepresentative results from binding experiments utilizing DMSO warrant further investigation. Thus, this study is dedicated to investigate the effect of using DMSO on the binding interactions between the truncated carbohydrate recognition domain (CRD) of the protein galectin-3 and the ligand KP0440 utilizing ITC and NMR.

## Isothermal Titration Calorimetry

ITC is a modern microcalorimetric method for determining reaction enthalpies between species in very small volumes. It operates by measuring the heat produced when precise amounts of reactants either engage or disengage in either covalent or noncovalent bindings, such as ligands interacting with protein molecules. The sample cell, along with a non-reacting reference cell are both heated with the same reference power. A feedback system is used which measures the difference in temperature resulting from the apparent reaction energy change, and adjusts the heat applied to the sample cell in order to retain equivalent temperature. The power requirement for this adjustment of heat to the sample cell is what is presented as a thermogram (PEAQ-ITC Manual, 2015). If the reference power needs to be lowered in the sample cell to retain equal temperature to the reference cell, it means that the reaction releases heat i.e exothermic, and if the reference power needs to be increased, it in turn indicates that the reaction is endothermic. It is of import to mention that ITC only measures the global energy change of the sample cell, including both the reaction of interest as well as other possible undesired side reactions. It is therefore of critical import to ensure that the reaction solution is prepared in a way to avoid cross reactions (C. Ráfols et. al, 2016). The area of the injection peaks in the thermogram can be plotted against the molar ratio of protein and ligand in order to obtain a reaction isotherm. A schematic representation of a reaction isotherm is presented in Figure. 1, where it is shown that the difference in energy between the the initial stage of the reaction and close to saturation can be related to apparent enthalpy.

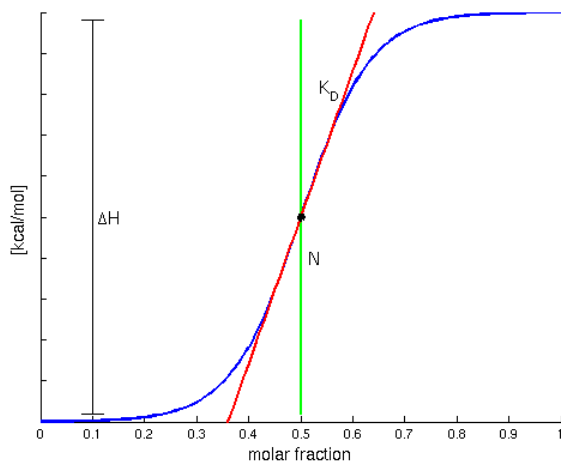


Figure 1 shows a schematic representation of an binding isotherm from an ITC thermogram (blue), along with some discernible parameters. The midpoint of the titration curve relates to the binding stoichiometry (green), the inclination is related to the dissociation constant (red), and the difference in energy between the bound and unbound state can be related to the apparent enthalpy of binding (black).

The energy release/absorption of an injection is provided by equation 1:

$$\Delta Q(i) = Q(i-1) + \frac{V_t}{V_0} \frac{Q(i)-Q(i-1)}{2} + Q_{off} \quad (1)$$

Where  $V_t$  is the injection volume,  $V_0$  is the volume of the cell,  $Q_{off}$  accounts for eventual buffer mismatch causing erroneous heat contributions, and  $\Delta Q(i)$  is the heat difference after injection  $i$  (Freiburger, 2015). The dissociation constant  $K_D$ , the binding stoichiometry  $n$ , and binding enthalpy  $\Delta_b H$  are calculated by fitting the data to equation 2:

$$Q(i) = \frac{\Delta_b H + V_0}{2} [a - \sqrt{a^2 - 4nM_i X_i}] \quad (2)$$

$$\text{Where } a = nM_i + X_i + K_D \quad (3)$$

Where  $M_i$  and  $X_i$  are the concentrations of protein and ligand during injection  $i$  respectively.  $K_D$  along with the temperature can be related to the standard free energy using equation 4, where  $R$  signifies the ideal gas constant, and  $T$  the temperature.

$$\Delta_r G^\circ = -RT \ln\left(\frac{1}{K_D}\right) \quad (4)$$

This is the free energy difference between the bound state and the free state during standard conditions. The enthalpy resulting from equation 2 is the energy released as  $M_i$  moles of protein react with  $X_i$  to reach their equilibrium concentrations. This enthalpy is converted into the standard enthalpy for the binding event by equation 5:

$$\Delta_r H^\circ = \Delta_b H \frac{c_p}{[PL]} \quad (5)$$

Where  $c_p$  is the total concentration of protein in the sample, and  $[PL]$  is the concentration of ligand-bound protein. This along with the standard free energy can be used to calculate the standard entropy according to equation 6:

$$T\Delta_r S^\circ = \Delta_r H^\circ - \Delta_r G^\circ \quad (6)$$

Where  $T$  is the temperature. This method for obtaining a complete picture of the reaction thermodynamics makes ITC a powerful tool for characterization of reactions in terms of energetics (Falconer, 2010).

## Basic Concept of Nuclear Magnetic Resonance Spectroscopy

NMR is along with X-ray crystallography the two most common techniques that allow for three dimensional conformational data of high molecular weight substances at high resolution (Cavanagh, 2007). NMR is based on nuclear spin, an inherent characteristic of atoms, which allows the nuclei to act similar to magnets. This characteristic is described by a spin number, designated  $I$ , and only nuclei with nonzero spin numbers can be observed in NMR, such as  $^1\text{H}$ ,  $^2\text{H}$ ,  $^{13}\text{C}$ , and  $^{15}\text{N}$  for instance. In a NMR experiment, the sample is placed within a powerful magnetic field that is homogeneous across the relatively small sample tube. The spin moments of the nuclei with nonzero spin numbers will then begin to precess around the applied field at a due to the torque generated from the interaction between the spin momentum and the field itself. The bulk magnetization,  $M_0$  is the vector sum of all individual spin moments which will be aligned with the applied static field, and parallel to it for nuclei with positive gyromagnetic ratios,  $\gamma$ , and a characteristic constant for each type of isotope. The individual spin moments will precess along the z-axis, making each direction in the xy-plane equally probable, resulting in the transverse component of  $M_0$  averaging to zero. This is referred to as the equilibrium state. NMR signal is acquired when this state is disrupted, for instance by applying a radio pulse,  $B_1$ . If this pulse is of a resonance frequency, i.e a wavelength that corresponds to a specific type of nucleus, it will effect these nuclei. The pulse is applied orthogonally with respect to the base magnetic field. This occurs in what is referred to as the ‘‘rotating frame’’. The rotating frame is a coordinate system where the xy-

plane rotates around the z-axis at a frequency equal to the intrinsic precession frequency of the nuclei called the Larmor frequency. This frequency is much larger (~MHz) than the chemical shifts of interest (~kHz) and is compensated by the rotating frame in order to allow for NMR measurements. The pulse will rotate the bulk magnetization clockwise along the axis of the applied pulse, generating a transverse component of the bulk magnetization. This magnetization will decay as the bulk magnetization will return towards to the equilibrium state while precessing around the z-axis. This is referred to as relaxation (Derome, 1987). The transverse magnetization induces a current in the coil which acts as the signal for NMR experiments. This signal contains information of both chemical as well as conformational structure and is referred to as Free Induction Decay (FID) (Cavanagh, 2007). This signal can via Fourier transformation be converted from the time based domain to a frequency based (Hz or Rad) spectrum (Figure 2).

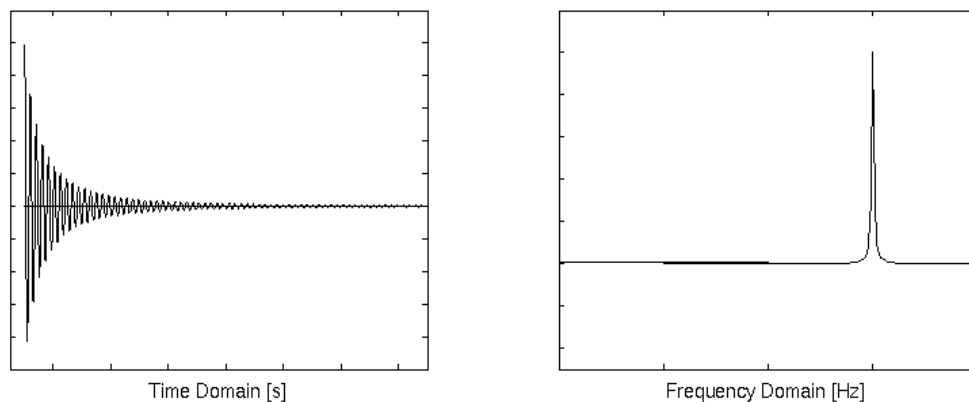


Figure 2 shows a schematic representation of a Free Induction Decay signal (left) and the Lorentzian peak resulting from Fourier transformation.

These frequency domain spectra are proportional to the homogeneous field, and is commonly normalized to allow comparison between magnetic field strengths, i.e different spectrometers, according to equation 7:

$$\delta(ppm) = 10^6 \frac{\nu - \nu_{ref}}{\nu_{ref}} \quad (7)$$

Where  $\nu$  is the frequency of the peak, and  $\nu_{ref}$  is the frequency of a reference compound. As the ratio of two frequencies are compared the field dependence is removed. This makes the spectra more easily interpretable and allows for varied study of many different spin systems, such as the chemical exchange between two states (Kleckner et al., 2011).

## CPMG

Carr-Purcell-Meiboom-Gill is a specific sequence of pulses utilized in pulsed NMR experiments for studies of processes on millisecond timescales, such as protein conformational changes or association/dissociation dynamics. These types of mechanisms cause changes in chemical shifts which in turn affect the measurable relaxation in the transverse plane. During CPMG experiments the transverse relaxation  $R_2$  is measured, which is dependent on the chemical exchange  $k_{ex}$ . The most basic example of a CPMG pulse sequence is carried out by first applying a  $90^\circ$ -pulse followed by a period  $\tau_{CP}/2$ , after which a  $180^\circ$ -pulse is applied followed by another period  $\tau_{CP}/2$ , which is repeated a varied number of times (Figure 2).

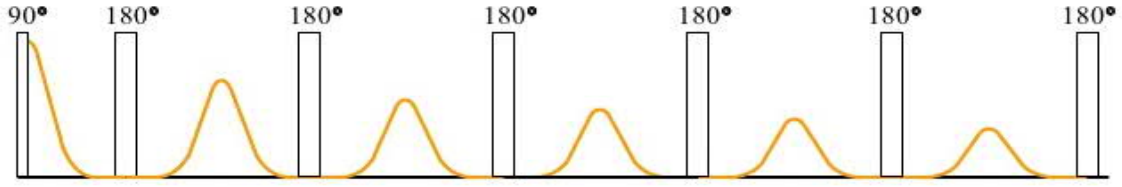


Figure 2 shows an example of the pulse sequence used for CPMG experiments, where the period between each 180°-pulse is  $\tau_{cp}$ . The picture shows the pulses applied which can be repeated  $n$  times, and yellow line picture shows the resulting signal, where the signal will decay as subsequent spin echo trains continue.

This  $\tau_{CP}$ -180° block is referred to as a “spin-echo” and refocuses the transverse magnetization. Varying the length of the period  $\tau_{cp}$ , i.e the amount of the spin-echo blocks during a constant period of time  $T_{CP}$ , provides varying times for the transversal relaxation. Calculating the transverse relaxation as a function of the pulse frequency,  $\nu_{CPMG}=1/(4\tau_{CP})$ , is performed by fitting the experimental data to equation 8:

$$R_2 = -\frac{1}{T_{CP}} \frac{\ln(I(\nu_{CP}))}{I_0} \quad (8)$$

Plotting this yields a relaxation dispersion curve which can be fitted to equation 9 in order to relate the difference in chemical shift between the bound and unbound state to the chemical exchange rate of the reaction (Rules p. 416, 2006. Palmer, 2001):

$$R_2 = \frac{1}{2}(R_{2,A} + R_{2,B} + k_1 + k_2) - \left(\frac{1}{\tau_{cp}}\right) \ln(\lambda^+) \quad (9)$$

$$\lambda^+ = \frac{1}{2} \cosh^{-1}(D_+ \cosh(2\varepsilon) - D_- \cos(2\eta)) \text{ Where,}$$

$$D_{\pm} = \frac{1}{2} \left( \pm 1 + \frac{\psi + 2\Delta\omega^2}{\sqrt{\psi^2 + \zeta^2}} \right), \quad \varepsilon = \frac{\tau_{cp}}{\sqrt{8}} \sqrt{(+\psi + \sqrt{\psi^2 + \zeta^2})}$$

$$\eta = \frac{\tau_{cp}}{\sqrt{8}} \sqrt{(-\psi + \sqrt{\psi^2 + \zeta^2})}, \quad \zeta = 2\Delta\omega(R_{2,A} - R_{2,B} + k_1 - k_2)$$

$$\psi = (R_{2,A} - R_{2,B} + k_1 - k_2)^2 - (\Delta\omega)^2 + 4k_1k_2$$

The protein-ligand interaction is deemed to occur in the fast regime ( $k_{ex} \gg \Delta\nu$ ), where equation 9 can be simplified to equation 10:

$$R_2(\nu_{CP}) = R_2^0 + \left(\frac{p_A p_B (\Delta\omega)^2}{k_{ex}}\right) \left(1 - \left(\frac{4\nu_{CP}}{k_{ex}}\right) \tanh\left(\frac{k_{ex}}{4\nu_{CP}}\right)\right) \quad (10)$$

From equation 10, the chemical exchange rate can be determined for residues located in the binding site and corresponds to the association and dissociation of the ligand. The chemical exchange rate can be further extrapolated in the on- and off-rates (in units  $[M^{-1}s^{-1}]$  and  $[s^{-1}]$  respectively) of ligand binding according to equation 11-12:

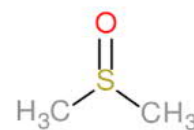
$$k_{off} = k_{ex}(1 - p_b) \quad (11)$$

$$k_{on} = \frac{k_{off}}{K_D} \quad (12)$$

Where  $k_{on}$  is the second order rate constant for the ligand binding into the protein,  $p_b$  is the concentration of free protein, i.e  $1-p_b$  is the relative population of bound protein,  $K_D$  is the dissociation constant, and  $k_{off}$  is the first order rate at which the ligand leaves the protein with the unit  $s^{-1}$ .

## Dimethyl Sulfoxide

DMSO is an organic compound consisting of a sulfur monoxide group bound to two methyl groups as seen in Figure. 3. It is commonly used as highly polar aprotic solvent. Its ability to solubilize both organic and inorganic compounds allows for solvation of a variety different analytes. This, along with its low toxicity makes DMSO attractive for many different laboratory applications, among them ITC and NMR. But there are also some setbacks as DMSO increases viscosity when mixed with (or dissolved in) water (J. Catalán et al, 2001). DMSO possesses significant hygroscopic tendencies, which can cause difficulties when requiring precise DMSO concentrations in solutions. It has been shown that DMSO displays water uptake from its environment over time and although this occurs over a long time period even slight differences in water content can have significant effect on solution viscosity, especially for low water content DMSO solutions (LeBel, 1962).



Dimethylsulfoxide (DMSO)

## Galectin-3C

Galectin-3 is a part of the lectin family which binds  $\beta$ -galactoside sugars, such as galactose. In this study, the mutant Galectin-3C (Gal-3C) was used, which is a truncated version of the the wild type protein only retaining the carbohydrate binding domain (CRD) of ~130 amino acids (PDB code: 3ZSJ), thus consisting of residues 113-246 of the untruncated protein (Dumic et al., 2006). Gal-3C mainly consists of two antiparallel beta-sheets, one of which acts as the binding site of the protein ranging from around residues 140-180 (Figure 4). The binding site is located in close proximity to the solvent making binding affinity highly dependent on solvent characteristics such as viscosity.

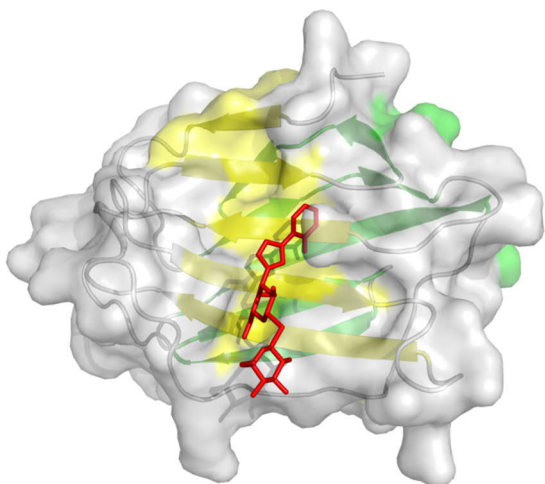


*Figure 4 shows an experimentally derived crystal structure of the binding interface of the carbohydrate recognition domain of galectin-3 (gray) with its two  $\beta$ -sheets colored yellow and green. The ligand KP0440 is colored red.*

## KP0440

The ligand used for this study is a phenyltriazolyl-thiodigalactoside with a fluoride at the ortho- position of the aromatic ring. A schematic representation of KP0440 is presented in Figure 5. KP0440 displays high affinity in Gal-3C binding (in the  $\mu$ M range), making it suitable for ligand-affinity studies of Gal-3C (Peterson et al., 2018).

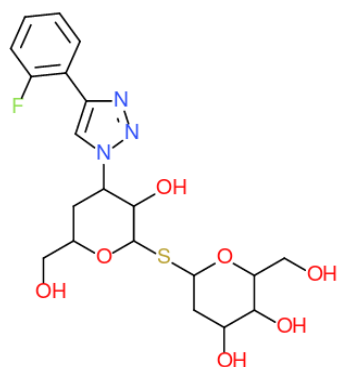


Figure 5 shows schematic a representation of the ligand KP0440 which was utilized in the project.

## Aim of the study

The aim of this thesis is to examine the effect of DMSO on the thermodynamics and kinetics of KP0440 binding to Gal-3C. The effect of DMSO on thermodynamics is studied by ITC, and the effect on kinetics is studied by NMR relaxation dispersion.

## Materials and Method

### Instruments

The MicroCal PEAQ-ITC system located at the Department of Biophysical Chemistry at LTH was used for the ITC experiments. The ITC instrument was connected to a computer in the lab which was used for data acquisition. Further computer analysis of the ITC raw data was performed using four open source programs, ConCat32, NITPIC (Keller, 2012), SEDPHAT, and GUSSE (Brautigam, 2015). ConCat32 is used for combining thermograms, NITPIC is used for peak integration, SEDPHAT for data fitting, and GUSSE for plotting the data. Protein concentration determination was performed using an Agilent 8453 UV-visible spectrophotometer provided by the Department. NMR experiments were carried out using the 600MHz Agilent/Varian spectrometer which is fitted with a triple resonance probe, and is located at the Department of Chemistry at LTH.

### Procedure

The effect of DMSO on protein ligand interactions was studied using ITC in combination with NMR relaxation dispersion experiments. The experimental design of the thesis is described below. All experiments were performed at the Department of Biophysical Chemistry at LTH.

### Protein preparation

Preparation of the protein Gal-3C was carried out by dialysis. Stock solution of protein complex bound with lactose was poured into a porous filter which was submerged into a buffer solution of 5 mM HEPES pH 7.4. The filter allows for escape of smaller molecules while retaining the protein. The lactose will thus migrate out from the filter bag by osmotic pressure differences. The buffer solution was changed every 12 hours for 10 days after which the filter bag containing the purified protein was drained into a falcon tube and put in cold storage until further use.

### Determination of protein concentration

Concentration determination of the purified protein solution was performed by UV-spectrophotometry. For Gal-3C measurements, the extinction coefficient,  $\epsilon$ , has been determined to be  $\epsilon = 9970 \text{ M}^{-1}\text{cm}^{-1}$  at 280 nm earlier by other scientists at the Department. This value is used to relate absorbance and concentration according to Lambert Beer's law (equation 13):

$$A(280 \text{ nm}) = \epsilon lc \quad (13)$$

Where  $l$  is the length of the sample cuvette in cm,  $Abs$  is the absorbance value from the spectrophotometer at the wavelength 280 nm, and  $c$  is the protein concentration in mol/l. Protein sample were prepared by 20x dilution in HEPES 5 mM, after which the absorbance were measured and presented in Table 1. The resulting mean value was used as the concentration of the stock protein for following calculations.

*Table 1 shows the measured absorbance and resulting concentrations from the protein concentration determination experiments using spectrophotometry.*

Sample:	Abs [AU]	Protein concentration [mM]
1	0.35	0.71
2	0.38	0.77
Mean value:	0.37±0.021	0.74±0.042

## Preparation of sample solutions

### Protein and ligand concentrations

Preparation of samples for ITC measurements are performed by preparing 1.6 ml solutions of protein solved in HEPES buffer. The desired concentration is determined according to the rule of thumb presented in the manual for the ITC handbook (equation 14).

$$C = n \frac{M_{prot}}{K_D} \quad (14)$$

Where  $n$  is the binding stoichiometry,  $M_{prot}$  is the concentration of Gal-3C, and  $K_D$  is the dissociation constant. The value  $C$  is an arbitrary parameter which lie between 1 and 1000 in order to achieve an appropriate sample concentration.

### Preparation of DMSO dilution series for ITC experiment

In order to avoid the hygroscopic absorbance of pure DMSO under regular atmosphere as described in the theory section, a stock solution of 50% DMSO diluted with 5 mM HEPES buffer was prepared. From there 3 intermediate dilutions were prepared with concentrations 10%, 30%, and 50% DMSO. From these 0.4 ml were pipetted into the protein solution and 0.2 ml in the ligand solutions to a final volume of 2 ml for the protein solution and 1 ml for the ligand solution, achieving final DMSO concentrations of 2%, 6%, and 10%. The dilution was performed in this manner in order to reduce DMSO concentration mismatch.

### Preparation of NMR samples

Samples for the CPMG relaxation dispersion experiments were prepared according to Table 2 using the DMSO stock solution from the ITC sample preparation step for DMSO dilution. The final concentration of protein was adjusted to 400  $\mu$ M. D<sub>2</sub>O was added for signal locking, and the relation of protein/ligand was adjusted to achieve a saturation of 95% in order to increase sensitivity.

*Table 2 shows the sample preparation for the CPMG relaxation dispersion experiments*

	2 % DMSO	6 % DMSO	10 % DMSO
$V_{protein}$ [ $\mu$ l]	270	270	270
$V_{ligand}$ [ $\mu$ l]	14	13	21
$V_{DMSO}$ [ $\mu$ l]	20	60	100
$V_{D_2O}$ [ $\mu$ l]	50	50	50
$V_{HEPES}$ [ $\mu$ l]	146	107	59
$\Sigma$ [ $\mu$ l]	500	500	500



## ITC measurement

The ITC measurements were run in triplicates at 301 Kelvin, reference power at 10  $\mu\text{cal/s}$ , 750 rpm, initial delay of 60 s, initial injection volume 0.4  $\mu\text{l}$  followed by 9 injections of 4  $\mu\text{l}$  each. Following standard protocols, the duration of each injection (in units of s) was twice the volume (in units of  $\mu\text{l}$ ), resulting resulting in 0.8 s for the initial measurement and 8 s for the remaining injections. The experiment was carried out concatenating two runs into one, each with 10 injections fused into a single thermogram with 18 injections in total subtracting both initial injections. 300  $\mu\text{l}$  of protein solution was pipetted into the sample cell by inserting the loading syringe, then gently touching the bottom of the sample well, then raising it approximately 1 mm. The sample solution was then slowly dispensed into the sample well, with small volumes of sample being injected quickly intermittently in order to dislodge any eventual bubbles. Any excess sample will gather in an overflow cup above the sample cell, so that this volume is removed. 75  $\mu\text{l}$  of ligand solution was pipetted into a sample tube, upon which the ITC syringe will aspire the sample. After these steps, the ITC run was initialized. After the run was complete, the syringe was filled with new ligand solution in the same way as earlier, upon which another run was immediately started in order to allow for higher saturation of the protein. In addition to these runs, measurements carried out in the same way but halving the injection volume were carried out for 0% and 6% DMSO to receive more data points in the initial phase of the titrations yielding more statistically robust data. These baseline runs were carried out in duplicates. This means that three concentrations of DMSO along with a control results in 32 ITC runs in total. These runs were analysed using some computer softwares as described below.

## Data analysis of ITC measurements

The thermograms resulting from the ITC measurements were fed into Concat32, which yielded a concatenated thermogram from the two half-runs. These combined thermograms were then corrected for baseline differences, then fed into NITPIC. NITPIC integrates the peak areas of all replicates at once. This means that all datasets of a single DMSO concentration were fitted globally (Keller et al., 2012). These files were then fed into SEDPHAT, in order to fit the data to an isotherm. SEDPHAT calculated the thermodynamic profile, i.e values for  $K_D$ ,  $\Delta H$ , and  $\Delta S$ , for the thermogram as well as the precision of the fit. The free energy difference  $\Delta G$  of the reaction was calculated according to equation 4. Using the “automatic confidence interval search w projection methods” function in SEDPHAT yields the standard deviation of  $K_D$  and  $\Delta H$  according to F-statistics (Johnson et al., 1992). Errors of the remaining thermodynamic values were calculated via error propagation. The data was then fed into GUSSI in order to obtain graphical representations for presentation in this report (Brautigam, 2015). These images will be discussed below.

## NMR

In this report, 3 CPMG relaxation dispersion experiments were carried out in order to investigate the reason for the reduced binding affinity caused by an increase in DMSO concentration. NMR samples were prepared to a final protein concentration of 500  $\mu\text{M}$  saturated to 95% for 2%, 6%, 10% DMSO as described in the methods section. A CPMG pulse sequence was employed with a constant relaxation time of 40 ms and 16 values of  $\nu_{CPMG}=1/(4\tau_{CP})$  between 0-1000 Hz. Relaxation dispersion data for Gal3C-KP0440 at 0% DMSO available from earlier studies will be used as comparison in the discussion. NMR CPMG spectra were initially processed using NMRPipe (Delaglio, 1995) for resolution enhancement by multiplying the signal data with sine bell function, zero filling to acquire more points where no magnetization is detected, fourier transformation, phasing adjustment, and baseline correction. The peaks in the spectra were integrated in PINT (Ahlner, 2013. Niklasson, 2017) and calculation of  $R_2$  for each residue over each value of  $\nu_{cp}$  was carried out. The relaxation data are then exported to the Matlab program CPMG-fit written in-house, where values of  $R_2$  for each residue were fitted according to equation 10 in order to calculate values of  $k_{ex}$ ,  $p_A$ , and  $\Delta\delta$ .

# Results

## ITC measurements

DMSO dilution series of protein and ligand samples were prepared for ITC experiments in order to observe DMSO-related effects on reaction characteristics. Examples of the results of the ITC measurements are presented below in Figure 6. Each of the isotherms are one replicate each. All collected thermograms and associated binding isotherms are presented in Appendix A.

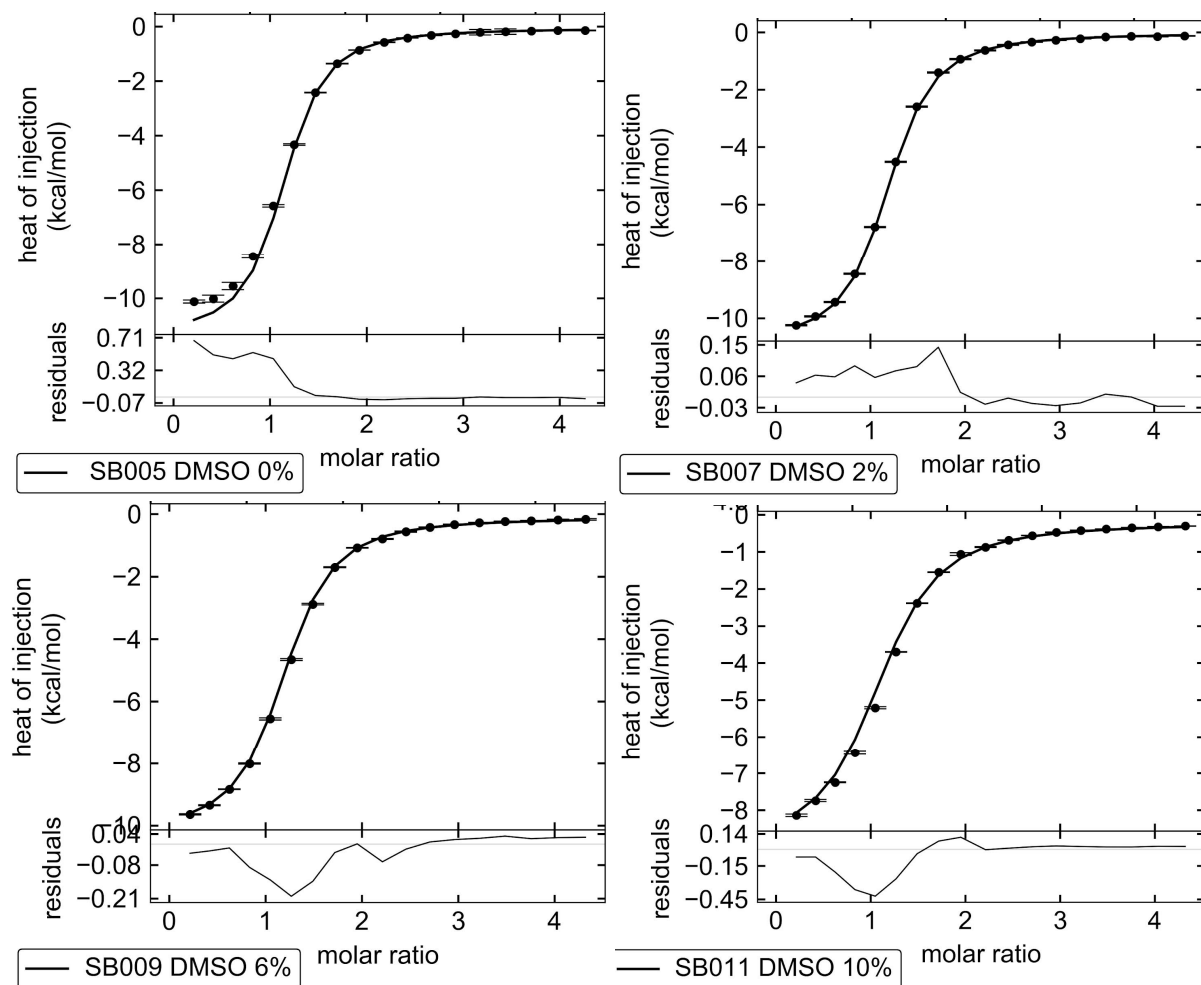


Figure 6. Characteristic examples of binding isotherms for the ITC experiments carried out during this project, each performed identically over the DMSO dilution series for 0% (top left), 2% (top right), 6% (bottom left) and 10% (bottom right). Each point in the binding isotherms represents an integrated peak in the corresponding thermogram.

From the resulting binding isotherms (Figure 6), dissociation constants,  $K_D$ , for each of the DMSO concentrations were determined and displayed in Figure 7 and Table 3.

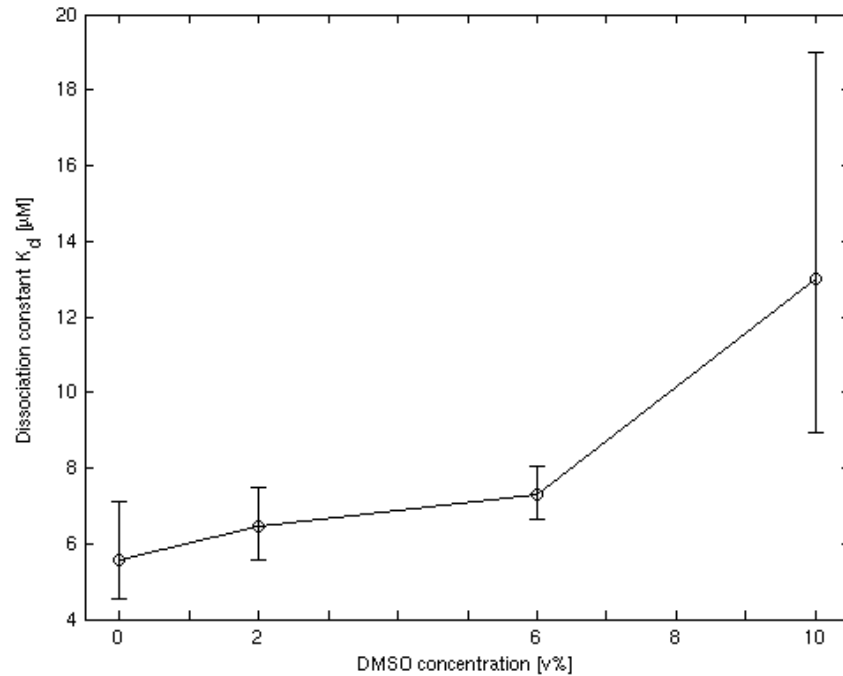


Figure 7. A graph of calculated  $K_D$ -values derived from the ITC experiments for each of the DMSO concentrations.

Table 3. Calculated  $K_D$ -values derived from ITC experiments for each of the DMSO concentrations, along with the average standard deviations of each parameter.

Volume percent of DMSO [v/v]	$K_D$ [ $\mu\text{M}$ ]
0%	5.6 <sup>A</sup> ± 1.3
2%	6.5 <sup>A,B</sup> ± 0.9
6%	7.3 <sup>B</sup> ± 0.7
10%	13.0 <sup>C</sup> ± 5.0

$K_D$  is shown to increase with each DMSO concentration. There is no significant difference between 2% and 6% DMSO. Thermodynamic data from the ITC runs of the DMSO dilution series are presented below in Figure 8 and Table 4.

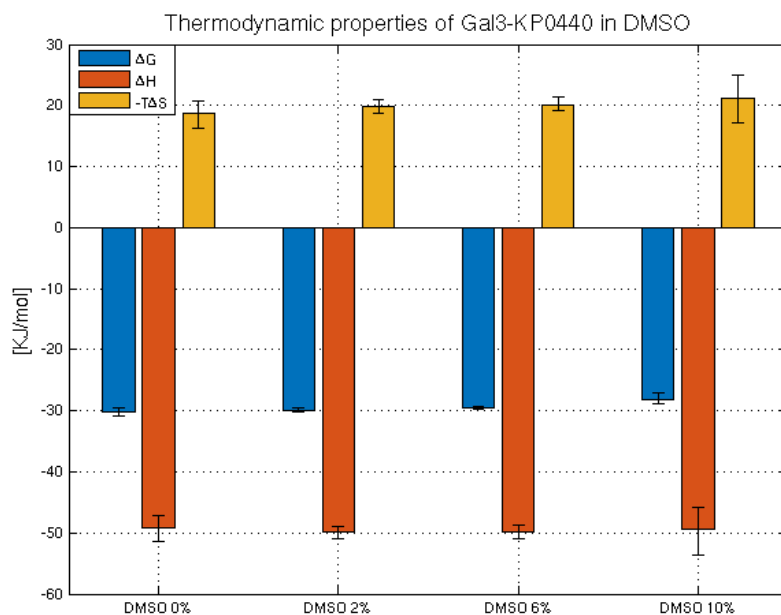


Figure 8. Calculated thermodynamic parameters for each of four DMSO concentrations (0%, 2%, 6%, and 10%). The yellow, orange, and blue bars represents  $-T\Delta S$ ,  $\Delta H$ , and  $\Delta G$ , respectively.

Table 4. Calculated thermodynamic parameters for each of four DMSO concentrations along with the average standard deviations of each parameter.

Volume percent of DMSO [v/v]	$\Delta G$ [kJ/mol]	$\Delta H$ [kJ/mol]	$-T\Delta S$ [kJ/mol]
0%	-30.3 <sup>A</sup> ±0.6	-49.1 <sup>A</sup> ±2.1	18.8 <sup>A</sup> ±2.2
2%	-29.9 <sup>B</sup> ±0.4	-49.8 <sup>A</sup> ±1.0	19.8 <sup>A,B</sup> ±1.1
6%	-29.6 <sup>C</sup> ±0.24	-49.8 <sup>A</sup> ±1.1	20.2 <sup>B</sup> ±1.1
10%	-28.2 <sup>D</sup> ±1.0	-49.4 <sup>A</sup> ±3.8	21.3 <sup>A,B</sup> ±4.0

$\Delta G$  as well as  $\Delta S$  is shown to increase with DMSO. There is no apparent effect on  $\Delta H$ . All measurements show significant differences in  $\Delta G$ , but the results are not as clear for  $\Delta S$ . Only 0% DMSO are significantly different from 6% but it is visible that the entropy decreases with DMSO. Overall there is a clear trend that  $\Delta G$  becomes smaller when DMSO is increased, and that the main contribution to this decrease is the increase in  $\Delta S$ .

## NMR

In order to further study the apparent decrease in binding affinity, CPMG experiments were performed for each concentration of DMSO. 12 residues located in close proximity to the binding site showed dispersions across all DMSO concentrations. Figure 9 shows representative relaxation dispersion profiles for three residues located in the binding site, while Fig. 10 shows examples for residues outside the binding site; all other dispersion profiles are presented in Appendix B. In both Figures 9-10 it is visible that  $R_2^0$  generally increases with DMSO for both dispersions located in and outside of the binding site.

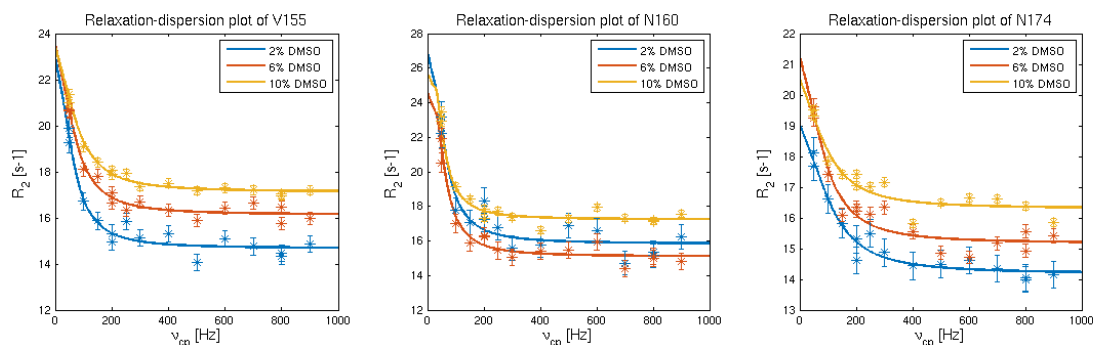


Figure 9. 3 characteristic dispersion plots for V155 (left), N160 (center), and N174 (right), all located in the binding site.

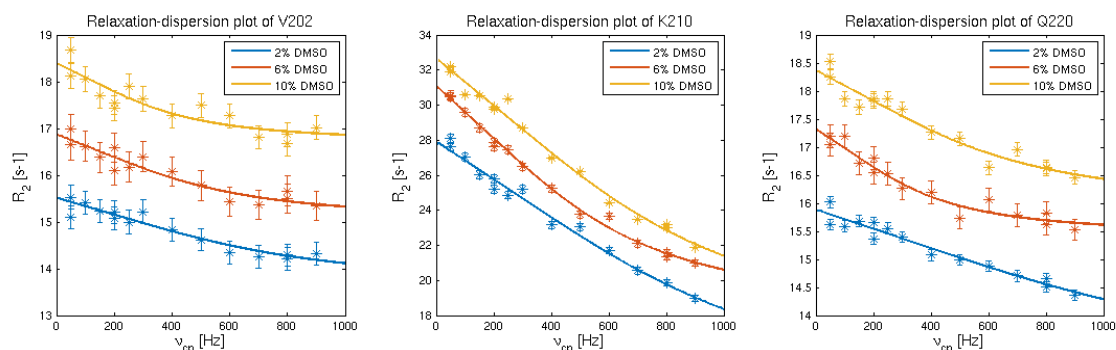


Figure 10. 3 characteristic dispersion plots for V202 (left), K210 (center), and Q220 (right), all located outside of the binding site in the  $\beta$ -sheet located on the opposite side of the binding site.

Figure 11 highlights those residues in the binding site that show exchange. The residues which displayed dispersions in the binding site are located around residues 140-180, placing them in the front  $\beta$ -sheet of the protein where the ligand binds. Evaluating the exchange rates of these dispersions should thus provide information of the binding kinetics of the protein-ligand interaction.

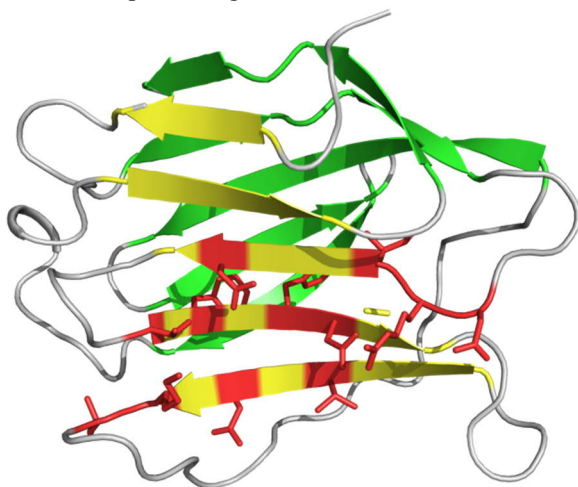


Figure 11. Graphical representation of protein the Gal-3C (gray) with the front  $\beta$ -sheet (yellow) and back  $\beta$ -sheet (green) highlighted with residues located in the binding site which displayed CPMG dispersions highlighted (red). These residues are N143, R144, I145, D148, V155, F159, N160, V172, N174, K176, and L177.

In order to determine whether the chemical exchange observed in these dispersions are caused by protein-ligand binding, the observed shift changes are plotted against shift differences between the bound and free (apo) states, for both 0% and 10% DMSO (Fig. 12). If the shift difference is completely caused by the binding event, each data point would be located on the diagonal line presented in the figure. Most of the residues displayed small shift change around

0.5 ppm with the exception of R144 where the measured shift change was  $\sim 1.3$  ppm. As for the theoretical shifts differences of binding, most residues generally showed smaller changes, but the shift difference for R144 was slightly higher.

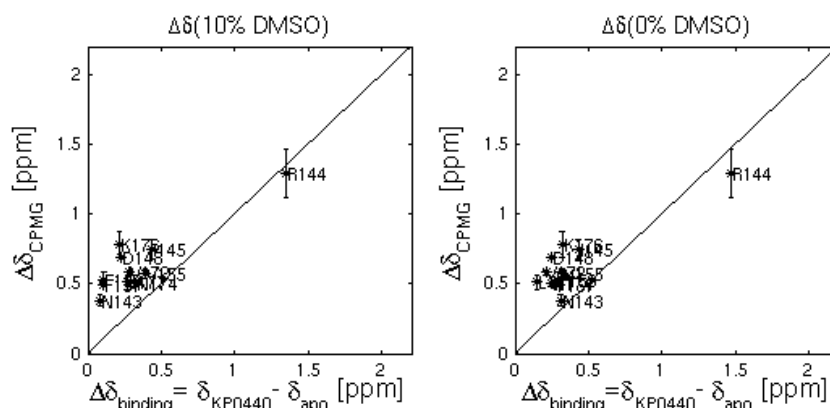


Figure 12. The chemical shift difference of the dispersible residues in the binding site plotted against calculated binding shifts difference for DMSO concentrations of 0% and 10%.

Performing a global fit of the 12 dispersions located in the binding site with the population of bound protein, exchange rate, and shift difference as free parameters (equation 10) yields the exchange rate constants presented in Figure 13. Utilizing equations 11-12 and the  $K_D$ -values derived from the ITC experiments yields the on- and off-rates of protein ligand binding in Figure 13.  $k_{ex}$ ,  $k_{on}$ ,  $k_{off}$  are all shown to decrease with DMSO.

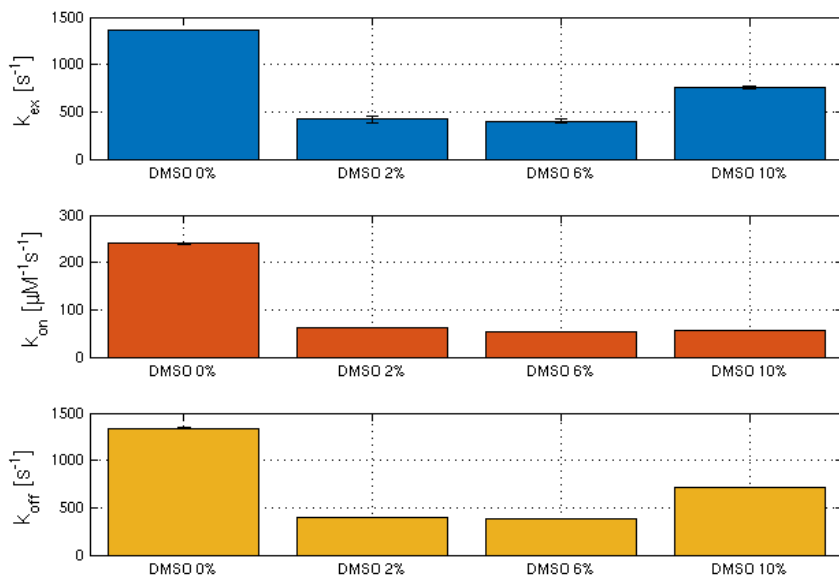


Figure 13. Calculated kinetics parameters as a result from the CPMG experiments as a function of DMSO concentration. The exchange rate (blue) are derived in CPMG-fit, the on-rate (orange) as well as the off-rate (yellow) are calculated using equation 11 and 12, respectively.

Exchange rates were fitted for dispersions located outside of the binding site as well. The residues which showed dispersions across the dilution series were located at the  $\beta$ -sheet on the opposite side of the binding site. These were A216, D215, G136, H208, K199, K210, Q220, V202, V204, and V213. No data for these residues were available for the 0% DMSO measurement that was provided for this study and is thus excluded. The results of the calculations for each measurement are presented in Table 5. It is clear from the results that the exchange rate is much higher outside of the binding site.

Table 5. Calculated exchange rate constants for the DMSO dilution series. The exchange rates are calculated using global fitting of the residues, both inside and outside of the binding site. The data provided for 0% DMSO did not display any dispersions outside of the binding site.

Global fit	DMSO concentration [v/v]	$k_{ex}$ [ $s^{-1}$ ]
Binding site	0%	1361.6±0.005
	2%	420.2 ±30.9
	6%	402.6 ±25.0
	10%	755.0 ±12.1
Outside of the binding site	2%	4039.0±285.0
	6%	2558.5±100.9
	10%	3925.4±66.3

## Discussion

The results of the ITC experiments in Figure 7 display a trend towards increasing  $K_D$  when the concentration of DMSO is increased indicating a negative effect on protein-ligand binding affinity. Viscosity increases with DMSO which would reduce the frequency of protein-ligand encounters in solution resulting in an apparent reduced binding affinity. Figure 8 presents the thermodynamic fingerprint of binding across the series of different DMSO concentrations. The free energy change is shown to increase with DMSO indicating less favorable protein-ligand binding as the concentration of DMSO is increased.

No significant change in enthalpy is visible, which would indicate that DMSO has little to no effect on the energy release when the titrant is added to the sample solution. The energy released, barring any potential buffer mismatch from sample preparation, should be a sum of energy from noncovalent bond formation between the ligand and protein and the disruption of solvent-solute interactions as a result of protein-ligand binding. This could potentially be explained if both of these components remain unchanged with the increased DMSO concentration, or if they both counteract each other, or if the energy of ligand desolvation is much smaller than that of the reaction enthalpy. There should be an energy contribution from the latter explanation as earlier studies showed that no DMSO molecules occupy the space in close proximity to the binding site (Wallerstein, 2018), but the observations provided in this study would indicate that this contribution is very small. Attempting to quantify the solvation enthalpy of the ligand in DMSO would be an interesting subject for future studies.

The observation that the entropy term ( $-T\Delta S$ ) becomes increasingly positive with increasing DMSO concentration also indicates that protein-ligand binding becomes less favorable. This apparent trend can possibly be explained by the increased ligand solvation in DMSO yielding a more favorable environment in solution for the ligand. Overall there are clear effects on the thermodynamics of binding caused by addition of DMSO. The detailed nature of this was examined during the CPMG experiments. These experiments were carried out in order to present a clearer picture of how the increased dissociation constant was affected by calculating the kinetic on- and off-rate as  $K_D = k_{off} / k_{on}$ .

In both Figures 9-10 there is a clear trend that  $R_{2,0}$  increases with DMSO. This can be explained by the increase in global correlation time brought on by the viscosity increase resulting in slower rotational diffusion of the protein as suggested by earlier studies (Wallerstein, 2018). Notably, this trend is broken for the residue N160 shown in Figure 9. This is hopefully rectified by recording new data utilizing a different static magnetic field strength. In Figure 10, dispersions of 3 characteristic residues outside of the binding site are presented. Several residues outside of the binding site displayed dispersions, but fitted exchange rates were too fast to be associated with the binding event, as is the case of the 3 presented in Figure 10. A global fit of these residues were performed in the same way as for the binding site residues, and the exchange rate constant was around 4000  $s^{-1}$ , about ten times higher than the ones associated with binding. These chemical shift changes are thus most probably not related to ligand binding. Possible explanations for this could be that these shift changes are related to weak transient DMSO interactions or slight protein conformation shifts, which could be of interest for future studies.

Figure 12 presents comparisons between observed shift differences to calculated shift differences caused by ligand binding. Overall the fit appears slightly lower than the ideal shift difference indicating that the shift difference might be caused by other factors than just the binding event. However, the good agreement observed for R144, which shows the largest shift difference, suggests that the scatter among the data with smaller shift differences might be due to the fact that CPMG experiments were performed at a single static magnetic field strength. This could also possibly be rectified by performing new measurements utilizing a different static magnetic field strength as described earlier. In Figure 13, fitted exchange rate constants, and kinetic on-/off-rates across the DMSO dilution series are presented. The exchange rate constant is observed to decrease with DMSO which is in line with earlier results indicating that DMSO reduces the binding affinity of Gal-3C.

A decrease in on-rate is apparent, which could be the result of reduced diffusion of reaction species due to the viscosity increase. Addition of 10% DMSO to a water solution results in a relative viscosity increase of ~20%, which is much lower than the effect observed on the on-rate (a decrease by  $\approx 75\%$ ), which indicates that other mechanisms are also involved. Other contributions to the reduced on-rate are thus probable such as the preferred solvation of the ligand in the bulk as shown in the ITC experiments, this is another possible area of interest for future studies. For instance, by performing further NMR studies of ligand-DMSO solutions and study possible interactions between the two. Another possible contribution to the decrease in  $k_{on}$  could be competitive binding of DMSO to binding site of Gal-3C. This is a possibility as the binding site is located at the surface, similar to hen egg-white lysozyme, which has displayed specific DMSO binding according to previous studies (Jóhannesson, 1997). This could be measured by additional NMR experiments such as measuring the potential NOE that would arise from specific DMSO binding. Bound DMSO may display two  $^1\text{H}$  peaks, one for each methyl group, whereas the methyl groups of freely solved DMSO would be chemically equivalent (Liepinsh, 1997). Observing specific binding of DMSO is unlikely as previous studies have proven that the binding affinity to Gal-3 is much weaker than ligand binding and unable to interfere (Wallerstein, 2018).

The off-rate is also decreased, which might be caused by the increase in viscosity as well. This would cause difficulty for the ligand successfully exiting the solvation shell resulting in reduced likelihood of ligand molecules dissociating from the protein and instead rebinding to the binding site, resulting in the lower apparent rate of dissociation. This is a possible explanation, although it is difficult to elucidate whether it is viscosity or solvation effects that contributes mainly to the decrease in off-rate. Both on- and off-rates decrease with DMSO concentration. Notably the decrease in on-rate is ~10% greater than the decrease in off-rate with the addition of DMSO, which would indicate that the mechanism dominating the exchange rate is related to the reduced number of protein ligand encounters.

## Conclusions

The primary aim of the study was to elucidate whether or not the presence of DMSO had any effect on the results when carrying out affinity studies between Gal-3C and KP0440. This was accomplished by ITC experiments which proved an observable decrease in binding affinity when the DMSO concentration was increased from 0% to 10% (v/v). The thermodynamics of this effect was also determined using ITC data analysis, where the free energy was observed to increase with contributions primarily from entropy whereas the enthalpy displayed no change. This indicates that DMSO solvation of ligands affect the binding characteristics resulting in misrepresentative data when compared to other solvents. There were a few potential explanations for the observed decrease in affinity, such as viscosity contribution of DMSO, but is unlikely to be the only contributing factor as the viscosity increase of 0-10% v/v DMSO is around 20% while the decrease brought on by this addition was roughly 60%. Another possibility could be preferential solvation of the ligand in DMSO causing less favorable protein binding. In order to investigate this issue further, additional ITC experiments could be performed where the thermodynamics of ligand solvation in DMSO could be quantified. This would be carried out by ligand titration into a sample cell DMSO solution but without protein. An important aspect to consider when designing this experiment is making sure to avoid the mixing enthalpy that occurs when DMSO is dissolved in water.



The secondary aim of the project was to further elucidate the nature of the effect that DMSO poses on protein-ligand interactions. In order to achieve this, CPMG relaxation dispersion experiments were performed to determine chemical exchange rates and further determine kinetic on- and off-rates for the ligand binding and release. It was observed that the addition of DMSO resulted in a decreased exchange rate constant as well as decreases kinetic on- and off-rates.

The trend was not fully realized in the exchange rate and off-rate as there was a slight increase when the DMSO concentration was increased from 6% to 10%, these results should be viewed as preliminary until we have performed additional measurements using different static field strengths in order to achieve higher statistical significance. Despite this, clear negative effects of DMSO on the exchange rate could be observed. Notably, the addition of DMSO in the sample seemed to have a greater effect on the on-rate than the off-rate, which would indicate that the lower frequency of protein-ligand encounters in the solvent was the main mechanism responsible for the decrease in apparent binding affinity. It is yet to be determined whether this is caused by the increase in viscosity, or some type of solvent effects, or a combination of the two.

Another area of interest for future experiments would be measurements using differently structured ligands to study the effect DMSO could potentially have on different binding conformations. Further analysis of the dispersions outside of the binding site would also be of great interest in order to determine whether these are caused by conformational changes as a result of induced fit, or if they are indeed caused by short-term DMSO binding. Lastly, this could be additionally studied by performing CPMG-experiments for apo-samples in DMSO and examining the resulting dispersions for exchange rates associated to DMSO binding interaction to the protein surface.

## References

- Ahlner, A et al. (2013). "PINT: software for integration of peak volumes and extraction of relaxation rates". *Journal of Biomolecular NMR*. Vol 56, issue 3, pp. 191-202.
- Bouchemal, K. (2008). "New challenges for pharmaceutical formulations and drug delivery systems characterization using isothermal titration calorimetry". *Drug Discovery Today*. Vol. 13. Numbers 21-22. Pages 960 - 972.
- Brautigam, C.A. (2015). "Calculations and publication-quality illustrations for analytical ultracentrifugation data". *Methods in Enzymology*. Vol. 562, pp. 109-134.
- Catalán, J. et al. (2001). "Characterization of Binary Solvent Mixtures of DMSO with Water and Other Cosolvents". *J. Org. Chem*. Vol. 66. Number 17. Pages 5846-5852.
- Cavanagh, Wayne J. Fairbrother, Arthur G. Palmer, III, Nicholas J. Skelton. (2007). *Protein NMR Spectroscopy: Principles*. 2nd Edition. 30 Corporate Drive, Suite 400, MA 01803, USA: Elsevier Academic Press.
- Cubrilovic, D et al. (2013). "Influence of Dimethyl sulfoxide on Protein–Ligand Binding Affinities". *Anal. Chem*. Vol. 85. Number 5. Pages 2724-2730.
- Delaglio, F. et al. (1995). "NMRPipe: A multidimensional spectral processing system based on UNIX pipes". *J. Biomol. NMR*. vol 6.
- Derome, Andrew E. (1987) "Modern NMR Techniques for Chemistry". *Tetrahedron Organic Chemistry Series*. Vol. 6. pp 1-280
- Dumic, J et al. (2006). "Galectin-3: An open-ended story". *Biochimica et Biophysica Acta (BBA) - General subjects*. Vol. 1760. Number 4. Pages 616-635.
- Falconer, R.J. (2010). "Survey of the year 2009: applications of isothermal titration calorimetry". *Wiley Online Library*.
- Freiburger, L.; Auclair, K.; Mittermaier, A. (2015) "Global ITC Fitting. Methods in Studies of Protein Allostery". *Methods*. Vol. 76. Pages 149–161.
- Jóhannesson, H. Denisov, P. V., Halle, B. (1997) "Dimethyl sulfoxide binding to globular proteins: A nuclear magnetic relaxation dispersion study". *Protein Science*. Vol. 6. Pp. 1756-1763.
- Johnson, M.L et al. (1992). "Parameter Estimation by Least-Squares Methods". *Methods In Enzymology*. Vol 210.
- Keller et al. (2012). "High-precision, automated integration of multiple isothermal titration calorimetric thermograms: new features of NITPIC". *Methods* Vol. 76 pp. 87-98.
- Kleckner, I. et al. (2011). "An introduction to NMR-based approaches for measuring protein dynamics". *Biochimica et Biophysica acta*. Vol 1814. Pages 942-968
- LeBel, R.G et al. (1962). "Density, Viscosity, Refractive Index, and Hygroscopicity of Mixture of Water and Dimethyl Sulfoxide". *Department of Chemistry, McGill University, and Physical Chemistry Division, Pulp and Paper Research Institute of Canada, Montreal, Canada*
- Liepinsh, E, Gottfried, O. (1997). "Organic solvents identify specific ligand binding sites on protein surfaces". *Nature Biotechnology*. vol 15. pp. 264–268.

- Malvern. (2015). PEAQ-ITC: user manual. Retrieved from: <https://jeltsch.org/sites/jeltsch.org/files/files/MicroCal-PEAQ-ITC-user-manual-English-MAN0573-01-EN-00.pdf>
- Niklasson, M et. al. (2017). "Comprehensive analysis of NMR data using advanced line shape fitting". *Journal of Biomolecular NMR*. Vol. 69, issue 2, pp. 93-99
- Palmer, A. G III, Kroenke CD, Loria JP. (2001). "Nuclear magnetic resonance methods for quantifying microsecond to millisecond motions in biological macromolecules". *Methods Enzymology*. Vol. 339. Pages 204-238.
- Peterson, K. et al. (2018). "Systematic Tuning of Fluoro-galectin-3 interactions Provides Thiodigalactoside Derivatives with Single-Digit nM Affinity and High Selectivity". *Journal of Medicinal Chemistry*. Vol. 61. Pages 1164-1175
- Ràfols, C et al. (2016). "The Ca<sup>2+</sup>-EDTA chelation as standard reaction to validate Isothermal Titration Calorimeter measurements (ITC)". *Talanta*. Vol. 154. Pages 354-359.
- Rules, G. S. (2006). *Fundamentals of Protein NMR spectroscopy*. Vol 5. Springer. P.O. Box 17, 3300 AA Dordrecht, the Netherlands.
- Sigma Aldrich. (2018). Dimethyl sulfoxide 276855. [online] Available at: [https://www.sigmaaldrich.com/catalog/product/sial/276855?lang=en&region=SE&gclid=EAIaIQobChMI7bacnpO63QIVy-F3Ch0j9gqdEAAYASAAEgKtbvD\\_BwE](https://www.sigmaaldrich.com/catalog/product/sial/276855?lang=en&region=SE&gclid=EAIaIQobChMI7bacnpO63QIVy-F3Ch0j9gqdEAAYASAAEgKtbvD_BwE) [Accessed 14 Sep. 2018].
- Wallerstein, J, Akke M. (2018). "Minute Additions of DMSO Affect Protein Dynamics Measurements by NMR Relaxation Experiments through Significant Changes in Solvent Viscosity". *Chemphyschem*.
- Wiggers, H.J et al. (2007). "Effects of organic solvents on the enzyme activity of *Trypanosoma cruzi* glyceraldehyde-3-phosphate dehydrogenase in calorimetric assays". *Analytical Biochemistry*. Vol. 370. Pages 107-114.